International Journal of Design & Nature and Ecodynamics
Vol. 20, No. 12, December, 2025, pp. 2849-2858
Journal homepage: http://iieta.org/journals/ijdne

Assessment of Water Erosion in the Houran Valley Using the Gavrilovic Erosion Potential Method and Geomatics Techniques

Ammar Y. Awad*, Kamal A. Al-Qayyssi, Ameer Mohammed Khalaf, Omar Naji Omer

Department of Geography, College of Education for Humanities, University of Anbar, Anbar 31001, Iraq

Corresponding Author Email: ammar_hydro@uoanbar.edu.iq

Copyright: ©2025 The authors. This article is published by IIETA and is licensed under the CC BY 4.0 license (http://creativecommons.org/licenses/by/4.0/).

https://doi.org/10.18280/ijdne.201211

Received: 4 July 2025
Revised: 4 September 2025
Accepted: 14 November 2025
Available online: 31 December 2025

Keywords:
Gavrilovic Erosion Potential Method, Iraq, remote sensing, soil erosion, Wadi Hauran

ABSTRACT

The research focused on studying and analyzing the Wadi Hawran basin, the largest dry basin in Iraq, located within the administrative borders of Anbar Governorate. The study aimed to build a geographical database that would identify the problems that the region's soils suffer from, most notably soil erosion. The Gavrilovic Erosion Potential Method (EPM) was applied to estimate soil erosion, and the natural characteristics of the basin were analyzed: slope, temperature, rainfall, and the effect of vegetation cover were analyzed in determining the volume of lost soil. The application of the EPM model revealed the presence of a risk in the severe erosion category concentrated in the western regions, where the slope degree increased by 1.7%, and the area was 306.6/km^2. As for the weak erosion category, it constituted the highest percentage at 44.11% and an area of 7917.07/km^2. The use of remote sensing techniques showed a high possibility of determining the amount of eroded soil in Wadi Hauran. Here, it was possible to create a spatial database in the form of maps and tables that would clarify the spatial distribution of areas exposed to erosion.

1. INTRODUCTION

Water erosion is one of the most important geomorphological processes that directly affects the development of landforms. It also poses a serious environmental challenge in fragile environments, leading to soil loss, deterioration of agricultural lands, and increased flood risks, as soils are considered the primary water storage line. The Hauran Valley, located in western Iraq, is one of the areas highly vulnerable to water erosion due to the natural conditions of the region. It witnesses a significant rise in temperatures of (0. 21) 0°C/decade [1], which is higher than the global average of (0.15) 0°C/decade [2].

Advances in remote sensing technologies have created practical tools and advanced statistical methods for studying water erosion, calculating its quantities, and identifying affected areas. These technologies provide accurate spatial data that contribute to the analysis and monitoring of environmental changes. The Gavrilovic model was used to calculate the magnitude of soil erosion, a key model for assessing water erosion. The model analyzes a set of factors that contribute to the aggravation of the soil erosion problem, such as topography, soil properties, climate, and land use. The importance of combining the Gavrilovic model with Geographic Information Systems (GIS) techniques and remote sensing data is highlighted in constructing accurate spatial maps that determine the severity of erosion and its spatial categories, enabling the development of integrated management strategies for water basins. Numerous local and international studies have proven the effectiveness of this combination. A recent study in the Ratka Valley Basin in western Iraq applied the Gavrilovic model using remote sensing data and GIS techniques; the basin areas were classified into five erosion severity categories, enabling the identification of remediation priorities and mitigation of environmental degradation [3].

At the regional level, the Admir-Izem Basin in Morocco was studied. Landsat-8 imagery and digital elevation models (DEM) were used with the Gavrilovic model. Annual soil losses were estimated at an average of 15.88 tons/hectare/year. The results showed that slope was the most influential factor [4]. On a global scale, a study conducted in the Loess Plateau in China demonstrated that combining the Gavrilovic model with remote sensing techniques can achieve high predictive accuracy and help develop long-term soil management plans [5]. Taken together, these studies indicate that this scientific approach is an effective tool not only for assessing water erosion but also for predicting its future levels in light of climate change and increasing human pressure on natural resources.

1.1 Research objectives

(1) Estimate the amount of eroded soil in the Wadi Houran basin using the Gavrilovic Erosion Potential Method (EPM), relying on parameters extracted from remote sensing and GIS data to achieve accurate spatial results.

(2) Analyze the relative influence of natural factors (topography, vegetation cover, soil properties, and climate) on water erosion rates, and determine the spatial distribution

patterns of these factors within the basin.

(3) Classify basin areas according to erosion risk levels and identify hotspots most susceptible to soil loss at the sub-basin unit level.

(4) Evaluate the impact of human activity, including agricultural expansion, overgrazing, and resource exploitation, on increasing erosion rates in the study area.

(5) Propose practical strategies to reduce water erosion, including engineering measures (such as small dams and earth barriers) and biological measures (reforestation and vegetation protection), to preserve soil as a fundamental natural resource.

(6) Establishing a spatial database that can be used in the future to monitor erosion changes and monitor the implementation of sustainable natural resource management plans.

1.2 Scientific hypotheses

This research hypothesizes that using the EPM model, supported by remote sensing data and GIS techniques, can provide accurate estimates of the volume of eroded soil in the Wadi Hauran Basin. It is also hypothesized that analyzing the natural factors affecting water erosion, such as topography, soil properties, vegetation cover, and climate, will identify the areas most vulnerable to soil loss and provide effective strategies to reduce erosion risks and conserve soil as a key natural resource in the region.

1.3 Study area

The Wadi Hawran basin is located in western Iraq within the administrative borders of Anbar Governorate and is considered one of the largest basins in the western Iraqi desert. Its area is about 17,945 km². The basin extends outside the Iraqi borders within the territories of Saudi Arabia and Jordan. The valley flows into the Euphrates River south of the Haditha District.

The basin's terrain is characterized by undulating terrain, ranging from isolated hills reaching approximately 949 m in height to dissected plateaus, in addition to alluvial plains formed by water sedimentation during flood periods. Its soil is deep and renewable, enhancing its potential for agricultural investment, particularly for wheat and barley cultivation. These lands have held significant environmental and agricultural importance for hundreds of years. This is due to the constant flow of water during the rainy period, which can be inferred from as evidenced by the resulting landforms. Furthermore, the presence of oases, floodplains, and pastures, particularly in the eastern parts, contributes to the formation of an integrated ecosystem deep within the Western Desert. The existing vegetation provides a diverse habitat for wildlife, from domesticated to predatory creatures. The region also occupies a strategic location for Iraq, forming a natural corridor extending towards the borders with Saudi Arabia and Jordan, enhancing its importance as a transit and communication area between urban centers and border areas, especially given the limited infrastructure in the Western Desert [6]. At present, the vegetation cover has declined dangerously as a result of soil erosion and the prevalence of drought. Astronomically, the basin lies between 32.18° and 34.0° north latitude, and between 39.20° and 42.55° east longitude, as shown in Figures 1 and 2.

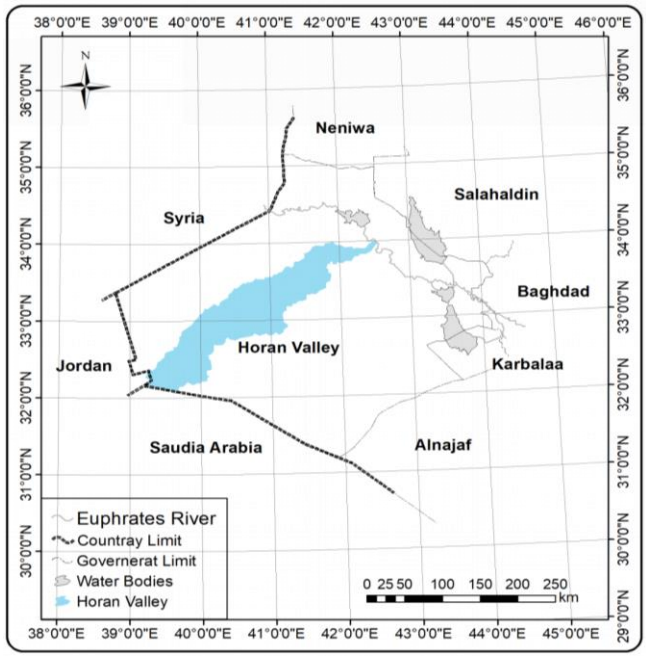

Figure 1. Location of the study area

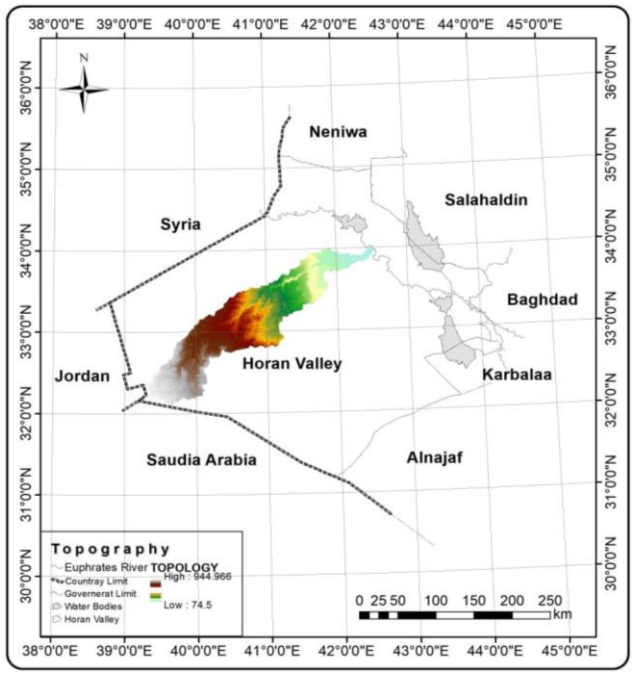

Figure 2. Topography of the study area

2. MATERIALS AND METHODS

Considering the vast area of the valley, which cannot contain all its boundaries within a single image, more than one satellite image with spatial accuracy (30 m) was used to cover the boundaries of the study area. The images were merged, and the boundaries of the study area were cut. These boundaries were obtained from the USGS website for the Landsat 8 satellite for the year 2024. All operations were carried out on them using the ArcGIS program.

The research is based on combining data derived from remote sensing with the application of a model. Gavrilovic for estimating the amount of water erosion of soils, through the following.

2.1 Data collection

Obtained Climate data (rainfall, temperature) from the NASA website for the year 2024 to assess their impact on erosion. Soil distribution maps and soil types were obtained from the Iraqi Ministry of Agriculture to assess their erosion susceptibility. Evaluate the impact of human activity, including agricultural expansion, overgrazing, and resource exploitation, on increasing erosion rates in the study area.

2.2 Application of the EPM

This model was developed during the 1950s and modified in subsequent years, and was applied to eroded areas in Italy, Switzerland, and Greece. It demonstrated great accuracy in estimating soil erosion through canals and cover erosion. After comparing the results extracted from the model with field measurements, a high degree of convergence was found in the model, indicating its potential for adoption in estimating soil loss in different regions. This, in turn, reduces effort and economic costs [7].

The EPM relies on remote sensing and GIS techniques to extract spatial values for the parameters affecting water erosion: slope factor, vegetation cover coefficient, soil erosion susceptibility coefficient, and rainfall factor. The process begins by collecting spectral, climatic, and geomorphological data from space and ground sources. Satellite images were then processed to derive slope and vegetation cover maps using spectral indices. In a GIS environment, each parameter is represented as a spatial layer with uniform spatial resolution. Spatial overlays are then performed to integrate these parameters into the model's main equation.

This process results in a quantitative estimate of eroded soil rates (m^3/km^3/year) for each spatial unit, with erosion severity classified into spatial categories that can be displayed on maps and analytical tables. This enables understanding of the spatial distribution of erosion risks and the development of appropriate management plans to mitigate them. The main equation is applied as follows [7, 8]:

$$W = H \times T \times \pi \times \sqrt{Z^3} \quad (1)$$

Since W is the annual rate of erosion (m^3/km_2/year), H is the annual rainfall rate (mm), T is the temperature coefficient, π is a constant value (3.1415), and Z is the erosion coefficient potential. It is extracted using the following equation [9]:

$$T = \sqrt{\frac{C}{10} + 0.1} \quad (2)$$

where, C is the annual average temperature.

It is considered that the Z-factor is one of the most important variables on which the Gavrilovic index depends, as it contains indicators that show the continuous and occurring changes in the study area, so it gives realistic results. It allows tracking and monitoring spatial changes in erosion levels over time and land use patterns. The Z-factor is extracted by the following [10]:

$$Z = Y \times Xa \times \left(\varphi + \sqrt{Ja}\right) \quad (3)$$

Since Y is the soil erodibility coefficient, Xa is the soil protection factor, φ is the erosion development coefficient, and Ja is the slope rate (%).

Erosion levels were classified according to the Z-factor values in Table 1. Gavrilovic highlighted some important indicators that illustrate the most significant factors revealing the changes occurring in the valley as a result of the changing values of these factors and indicators. Satellites were relied upon to estimate the final results of assessing the amount of erosion in the valley. Soil data were used to classify soils into three categories based on the physical and chemical properties and characteristics of the studied area. These factors were extracted from remote sensing data and the ArcGIS program. Then, the areas were classified according to the degree of erosion risk, and water erosion was estimated using the ArcGIS program's outputs.

Table 1. Potential erosion levels for Z-factor values

Erosion Level	Z
Very intense	> 1
Intense	1.0-0.81
Middle	0.80-0.41
Light	0.40-0.20
Very light	0.19-0.01

2.3 Extracting the potential erosion coefficient indicators

2.3.1 Soil erodibility index (Y)

It depends on the physical and chemical properties of the soil (texture, consistency, clay-sand ratio, organic matter content, and permeability). The higher the clay and organic matter content, the higher the soil's ability to resist erosion, while sandy or loose soils with weak cohesion are more susceptible to erosion. Y values are classified according to specific categories that link the degree of susceptibility to texture and cohesion properties.

The values of this index were calculated based on the soil map classified by the Iraqi FAO Company, which is a primary reference for determining the morphological characteristics of soil types in the study area. Laboratory analyses of field samples, including the chemical and physical properties of the soil, were also employed to determine the factors affecting its susceptibility to erosion. Studies indicate that the best apparent density for Iraqi soils is 1.20-1.40 g/cm^3 [11, 12]. The soils of the area were classified and divided into three groups (Table 2).

Table 2. Soil chemical and physical properties of the study area

No.	Depth (cm)	Percentage of Organic Material (%)	Fine Sand (%)	Fine Silt (%)	Clay Total (%)	Structure Type	Soil Permeability Moisture Percentage (%)
1	0.40	0.44	8.99	18.17	29.43	Granular	4
2	0.40	0.37	10.01	26.63	24.00	Platy	4
3	0.40	0.43	10.56	23.15	25.95	Finegranular	4

The following equation was applied to obtain the index values [10]:

$$Y = \begin{pmatrix} 0.00021 \times (12 - OM) M 1.14 + 3.25 \\ (S-2) + 2.5(P-3)/100 \end{pmatrix} \times 1.58 \qquad (4)$$

Since Y is the erosion coefficient, OM is the percentage of organic matter, M is the texture = (percentage of silt + fine sand) × (100 - percentage of clay), S is the structure symbol, and P is the permeability coefficient.

The obtained results are shown in Figure 3 and Table 3.

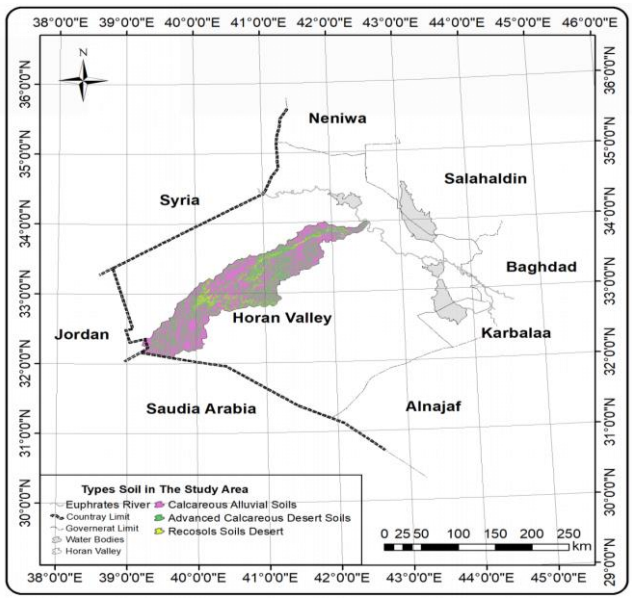

Figure 3. Soil types in the study area

Table 3. Erosion susceptibility coefficient y for the study area soil

Soil Type	Erosion Coefficient	Area (km^2)	Ratio (%)
Calcareous alluvial soils	Weak erosion	9064.85	50.52
Advanced calcareous desert soils	Moderate erosion	8000.15	44.58
Recosols soils desert	Severe erosion	880	4.90
Total		17000.945	100

2.3.2 Calcareous loamy soil group

The soils in this group are classified as (Je-10-2/3b) within the soil mapping unit, according to the FAO classification system (FAO, 2015).

Since:

Je = These are calcareous loamy soils that collect in valley bottoms and contain calcareous materials of no less than 50-805,

10 = the presence of linked soil units,

2 = represents the medium soil texture class,

3 = represents the fine soil texture class,

b = represents the simple undulating slope class with a slope degree of (0-8%).

The group of advanced calcareous desert soils and desert Recosols soils (Table 2 and Figure 3).

2.3.3 Soil protection index (Xa)

Xa represents the vegetation cover and its density. The coefficient values were extracted according to the vegetation cover values in the study area, which play a role in the soil erosion process. The plant works to limit the speed of water, which leads to a decrease in the amount of eroded soil if the vegetation is dense and vice versa. It is the rate at which rain falls on the Earth's surface.

Then, the collaboration was carried out in designing the cover based on the data of the Landsat 8 satellite imagery, where the bundle was effectively employed to derive the interactive factor of the robotic researcher. Then, its results were streamed into the EPM to estimate the soil protection index. This study combined remote sensing techniques and model analysis capabilities. It divided the Hauran Valley into five main categories of vegetation orientation ranges (Table 4), which enabled a quantitative spatial description of the extent of the contribution to reducing the percentage of variability in the desert and semi-arid environments.

Table 4. Standards for the soil protection factor (Xa) to Gavrilovic

Soil Protection Index	Value of Xa
Mixed forests - medium density	0.05-0.2
Pine forests and vegetation are scattered along the sides of the canals.	0.2-0.4
Fertile pastures	0.4-0.6
Degraded pastures	0.6-0.8
Barren lands	0.8-1.0

To accurately determine vegetation cover values, the NDVI equation was applied to extract the Xa index (soil protection index), focusing only on the winter season due to the region's dry continental climate, where rainfall is limited during this season and nonexistent during the summer. The absence of rain in the summer practically eliminates rain erosion, making the analysis of vegetation cover in the winter more realistic for assessing the role of plants in soil protection. linking the NDVI results to the EPM model outputs, showing that areas with high vegetation density recorded low erosion rates due to reduced runoff velocity and the mitigation of raindrops.

Meanwhile, areas with low vegetation cover exhibited high erosion rates, reflecting the close correlation between remote sensing data and the erosion indices calculated by the model. The results of which we can use to extract the Xa index values using the following equation [13]:

$$NDVI = \frac{NIR - RED}{NIR + RED} \qquad (5)$$

The near-infrared (NIR), the fifth spectral band of the Landsat-8 OLI sensor, is one of the most important spectral indices used in vegetation analysis. The red (R) and near infrared (NIR) bands, typically represented as Band 5 and Band 4 in certain sensors (e.g., Landsat 8), are used to calculate the Normalized Difference Vegetation Index (NDVI). This is one of the most widely used spectral indices for monitoring and assessing vegetation health and density. NDVI values range from +1 to -1; positive values indicate the presence of vegetation cover, and vegetation density increases as the value approaches +1, while. Negative values are often associated with aquatic areas, as water absorbs near-infrared radiation at a greater rate than visible infrared radiation, resulting in negative NDVI values [14, 15]:

$$Xa = \left(Xa\,NDVI - 0.61\right) \times \left(-1.25\right) \quad (6)$$

Xa is the soil protection index, and $XaNDVI$ is the vegetation coverage index adjusted for the soil protection index.

The vegetation cover index was applied to satellite images for the year 2024. Positive values of the index represent dense vegetation cover, while negative values represent barren lands.

The study area was classified into five categories according to the Gavrilovic classification (Table 4). Noticing that the soil protection index Xa is high in areas with dense vegetation cover, which are mostly distributed in the eastern parts (Figure 4), and this is a result of the flatness of the surface. The deposition of soil and its continuous renewal, in addition to the high moisture content of the soil, provide a great opportunity for the germination process.

The coefficient recorded low values in areas devoid of vegetation cover or barren lands, which are usually found in the western parts as a result of the ruggedness of the region, the presence of rocky edges, and the thinness of the soil resulting from severe erosion. From the above, it is clear that the importance of vegetation cover in limiting soil erosion or reducing its severity is evident, as the area has little vegetation cover and weak resistance to erosion processes (Figure 4).

It is clear from the results of Figure 4 and Table 5 that the soil protection index categories varied across the study area. The weak protection category occupied the largest area, covering approximately 11,446.9 km² of the total area. This indicates the prevalence of areas highly susceptible to water erosion and their weak resistance to erosion.

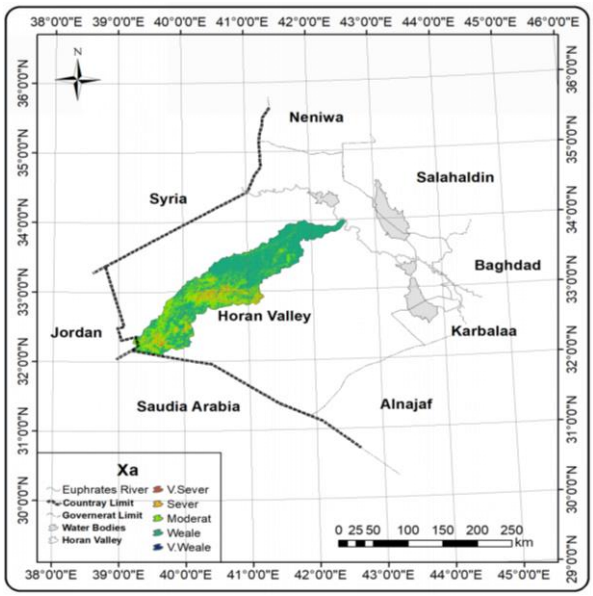

Figure 4. Xa factor

Table 5. Xa, area, and percentage of each category

Category	Area (km²)	Ratio (%)
Very intense	183.3	1.02
Intense	1598.2	8.90
Medium	4711.1	26.25
Weak	11446.9	63.78
Very weak	4.2	0.02
Total	17945	100

In contrast, the very weak protection category ranked lowest, with an area of only 4.2 km², reflecting its limited distribution.

These results indicate that most of the region's lands suffer from low levels of soil protection, underscoring the importance of vegetation cover as a key factor in reducing water erosion and maintaining soil stability.

2.3.4 Slope index (Ja)

The Wadi Hawran basin is characterized by a general slope extending from west to east, with its highest elevation reaching approximately 949 meters above sea level in the western part. In comparison, it gradually decreases to reach its lowest point at 80 meters above sea level in the eastern part, which represents the valley floor and its final outlet.

The topographic characteristics of the basin were analyzed using DEM data, which allowed for accurate slope values to be extracted within the study area. Elevation is a factor that directly affects water erosion processes, as steep slopes accelerate surface water flow, leading to soil fragmentation and its transport to lower areas via floods. The analysis results showed a direct relationship between the severity of the slope and the rate of erosion, with water erosion rates increasing in areas with high slopes, which are concentrated in the western parts, represented by isolated hills and rocky edges. Moreover, a decrease in flat and plain lands, which are distributed in the central and eastern parts, is represented by the oases, alluvial, and fan plains areas. Figure 5 illustrates the spatial distribution of the basin's slopes and their impact on water and soil movement, helping us understand the dynamics of hydrological processes that affect the sustainability of natural resources in the region.

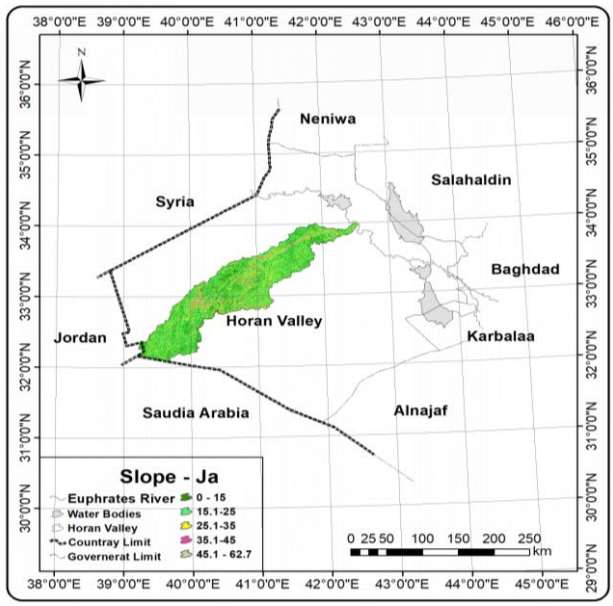

Figure 5. Slope index

From Table 6 and Figure 5, it is clear that the largest area of the valley is controlled by the weak and very weak categories, respectively. These areas represent the valley bottoms and plains, with areas of 8324.18 and 6060.07 km^{2,} respectively, and a percentage of 46.3% and 33.7%, respectively. The third place was occupied by the medium category, with an area estimated at 2772.43 km^2 and a percentage of 15.4%, as they represent the low hilly areas that are distributed in most areas of the valley. The fourth and fifth categories represent the areas of intense and very intense highlands, and they occupy an area estimated at 655.61 and 132.67 km^2, respectively. The percentages of 3.65% and 0.73% for each of them,

respectively, as these highlands represent areas of extreme erosion and drift due to height and lack of vegetation. In addition to the soil's ability to quickly disintegrate due to the original materials from which it was formed, there are the dry climatic factors in the region.

Table 6. Regression index area and percentage of each category

Category	Area (km^2)	Ratio (%)
very weak	6060.7	33.77
weak	8324.18	46.38
middle	2772.43	15.44
Intense	655.61	3.65
very intense	132.67	0.73
Total	17945	100

2.3.5 Current erosion index (φ)

This indicator illustrates the effect of land use (agriculture, grazing, urbanization) on soil erosion susceptibility. Exposed agricultural land or overgrazing reduces soil protection, while forests, natural pastures, and farms enhance soil resistance.

The index coefficients are extracted based on the satellite images of the Landsat 8 satellite through the attached table for the image by dividing the square root of the third band by the maximum radiation value (QMAX) as the relationship is directly proportional between radiation and erosion intensity (the radiation ratio increases with the increase in erosion intensity) as in the following equation [14]:

$$Q = \frac{\sqrt{TM3}}{QMAX} \tag{7}$$

where, $TM3$ is the third band in space visuals and $QMAX$ is the maximum radiation value.

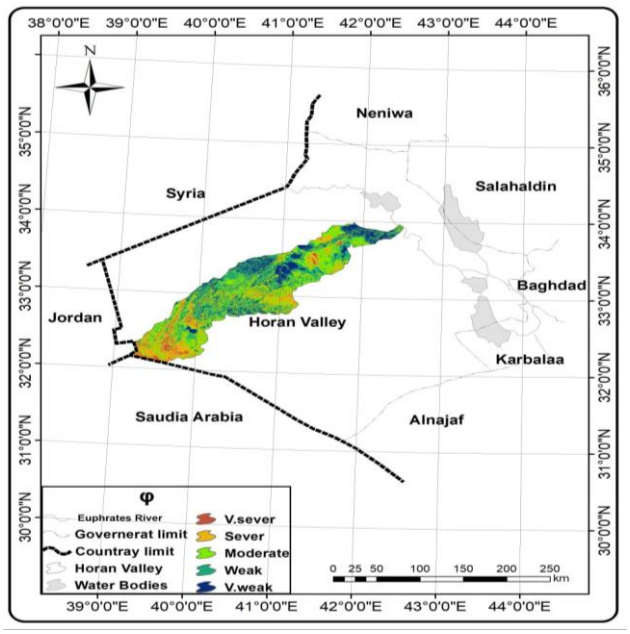

Figure 6. Land use

The values of these parameters are obtained from the metadata of the satellite imagery (Figure 6). The Houran Valley region is a remote area in the western plateau of Iraq. Its distance from urban centers contributes to the weakness of organized agricultural activity and the absence of effective land-use management. This emptiness allows for overgrazing, leading to the degradation of natural vegetation cover and increased soil vulnerability to exposure and erosion. Data on the erosion index (φ), extracted from Landsat 8 imagery, show high levels of radiation in the third band, reflecting the severity of erosion due to surface exposure and poor vegetation cover.

2.3.6 Potential erosion coefficient (Z)

It is considered the most important element in the Gavrilovic model, which was used to estimate the amount of soil eroded by water, as a value can be extracted from a group by combining all the previous indicators into a single, comprehensive mathematical formula that captures water erosion within the basin, the Z values were classified into five main categories to determine the spatial risk level. The results in Table 7 reveal the risk levels in the study area.

Table 7. Z-level categories, area, and percentage of each category

Potential Erosion Level	Area (km^2)	Ratio (%)
Very weak	1296.3	7.2
Weak	5776.1	32.18
Middle	6441.8	35.8
Intense	3558.6	19.8
Very intense	871.9	4.8
Total	17945	100

Figure 7. Potential erosion of the Z factor

The temporal and spatial variation of rainfall has a direct impact on hydrological activity [14, 15]. After the necessary transactions were combined to extract the values of the Z factor, Figure 7 was derived for the potential erosion in the Houran valley, where the smallest area was occupied by the category (very intense), with an area of 871.9 km^2 and a percentage of 4.8%. The largest area was occupied by the medium category, with an area of 6441.8 km^2 and a percentage of 35.8%. From the above, we note that all the extracted categories are distributed over all parts of the basin except for the steep category, which is confined to areas with a steep slope, and is represented in the middle parts of the valley, which are devoid of vegetation cover and extend from west to east. These results indicate that the Z-factor is an effective tool

for identifying areas most vulnerable to erosion and providing accurate spatial indicators to guide soil management strategies and reduce environmental degradation in the basin [16, 17].

2.4 Application of the EPM model to assess water erosion

As the model requirements must be analyzed, the auxiliary indicators are as in Eq. (1) [7, 8].

2.4.1 Rainfall index (H)

Rainfall is one of the most prominent factors controlling the intensity of water erosion in the Wadi Hauran Basin. Its kinetic energy directly affects the transport of soil from high and sloping areas to lower parts. The scarcity of vegetation exacerbates this process, allowing more soil to be eroded by surface runoff [18]. Given the vast area of the basin and the lack of local climate stations covering all its parts, we relied on NASA data available at http://chrsdata.eng.uci.edu, where spatially distributed points were selected to provide accurate data on rainfall amounts [19]. The results showed that the annual rainfall average during the study period was approximately 125 mm. Figure 8 shows a relatively low average [20]. However, its danger lies in the form of short, high-intensity rainstorms, rather than the length of the rainy season. This rainfall pattern is one of the key inputs into the rainfall coefficient calculations in the EPM model, which is used to estimate erosion rates. The model shows that the intensity of rainstorms, more than the total amount of precipitation, is the decisive factor in determining soil loss rates, thus contributing to explaining the spatial variation in erosion levels in the basin.

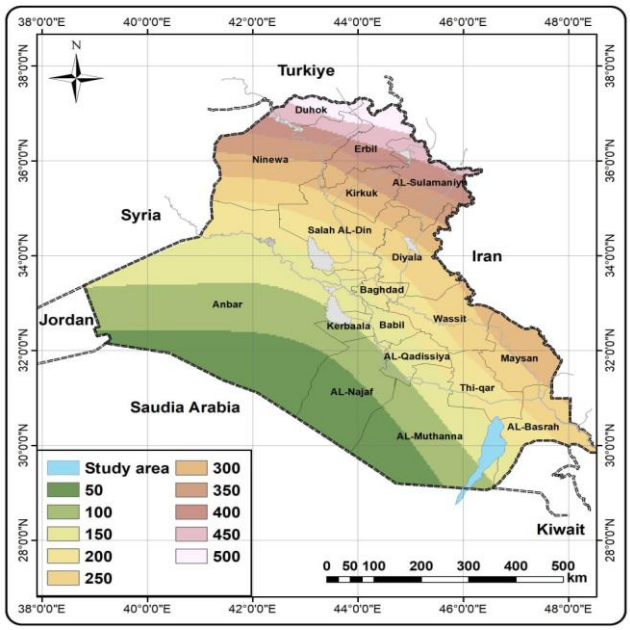

Figure 8. Rain equals lines

2.4.2 Temperature indicator (T)

The temperature index is an important factor for applying Gavrilovic's data, as it affects soils. High temperatures lead to increased evaporation, which leads to a decline in water quantities, which in turn causes the disintegration of soil and its components [15, 16]. High and low temperatures have a significant impact on the disintegration and fracture of rocks through the expansion and contraction of the minerals from which they originated, which facilitates their transport to another location by running floods. To obtain the average temperature during the study period, some equations were followed, as follows:

The numeric values (DN) of each pixel in the thermal infrared were converted to radiance values (DN to radiance) using the following equation [17]:

$$L_\lambda = M_L \times Q_{cal} + A_L \tag{8}$$

where, L_λ is the TOA spectral radiance (watts/(m^2·sr·µm)), M_L is the radiance multiplicative band (No.), A_L is the radiance add band (No.), and Q_{cal} is the quantized and calibrated standard product pixel values (DN).

The following equation was used to calculate the surface temperature [17]:

$$BT = \frac{K_2}{\ln\left(\frac{K_1}{L_\lambda}+1\right)} - 273.15 \tag{9}$$

where:

BT = Top of atmosphere brightness temperature (°C),

L_λ = TOA spectral radiance (watts/(m^2·sr·µm)),

K_1 is the constant band (No. 1), which is related to the thermal radiation emitted from the surface, and K_2 is the constant band (No. 2), which is used to adjust the logarithmic relationship between radiation and temperature.

All this data is contained in the metadata of the satellite imagery.

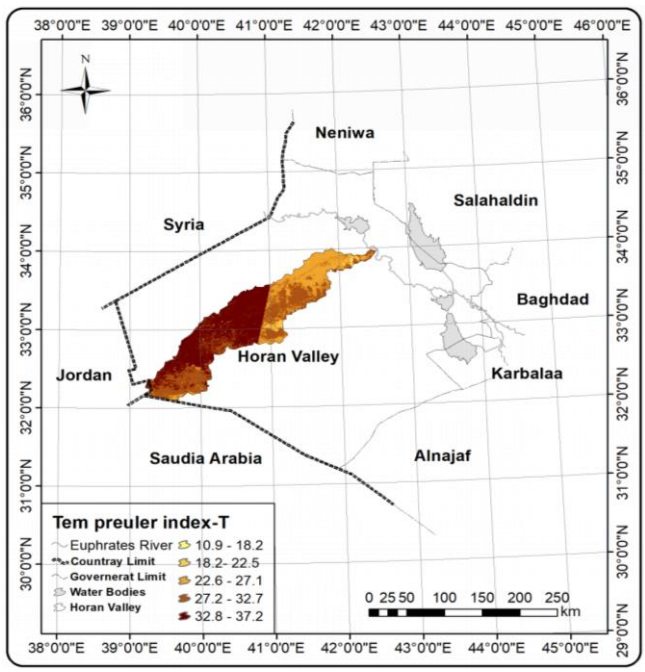

Figure 9. Annual average of the T factor for the Houran valley

Through Figure 9, it is clear that there is a variation in temperatures from the west of the study area towards the east. This is due to the topography of the area and its lack of vegetation, which contributes to higher temperatures. Additionally, the distance of the western region from water bodies helps moderate the atmosphere and lower the temperature.

2.5 Calculating the internal water volume using the EPM

Model Zachar [20] identified five types of water erosion based on the amount of soil in each, Table 8, to prepare a geographic database for Wadi Houran.

The valley was divided into five categories according to the amount of erosion, as the lowest amount formed by the category (very severe erosion) with an amount of 1210-7300 m^3/km^2/year, and an area of 306.6 km^2 with a percentage of 1.7%, while the largest amount formed by the category (weak) with an amount of 573-50 m^3/km^2/year and an area of 7917.07 km^2 and a percentage of 44.11% (Figure 10 and Table 8).

Table 8. Volume of lost soil and its percentage according to the EPM model

Category	Volume of Lost Soil Severity of Erosion (m^3/km^2/year)	Severity of Erosion	Area (km^2)	Ratio (%)
1	>50	Very weak erosion	4020.6	22.4
2	573-50	Weak erosion	7917.07	44.11
3	831-573	Moderate erosion	4297.2	23.9
4	1200-831	Intense erosion	1403.2	7.8
5	7300-1210	Very intense erosion	306.6	1.7
	Total		17945	100

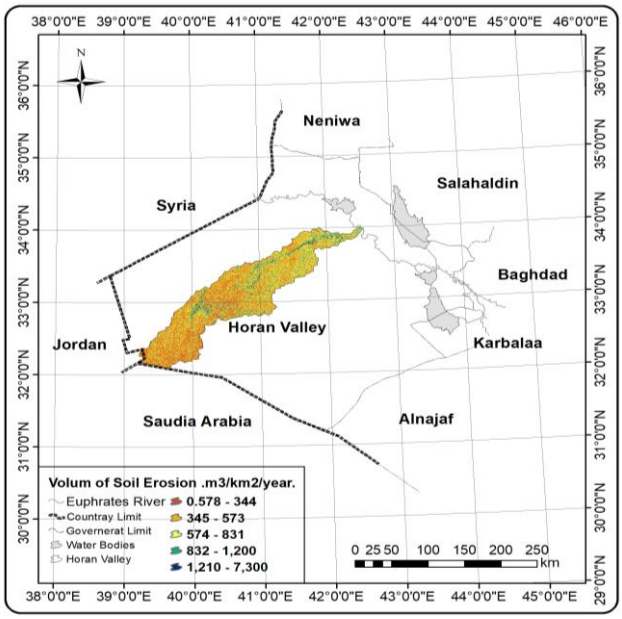

Figure 10. Erosion levels according to the amount of drift in the Houran valley

3. RESULTS AND DISCUSSION

Applying the Gavrilovic model demonstrated high efficiency in estimating the amount of eroded soil and determining the levels of water erosion intensity in the study area. This model calculates the erosion volume per pixel and relies on various factors in its calculations. The model revealed five types of water erosion in the basin, ranging from very weak to very strong, distributed across different areas of the basin.

The soil protection index (Xa) was extracted by analyzing satellite images, where the NDVI values extracted from Landsat images were combined with the raw Xa values, and the results were then fitted according to the criteria specified in the EPM Model. The results showed that the soil protection index (Xa) values ranged from 1.7% for the very intense category with an area of 306.6 km² to 44.11% for the weak category with an area of 7917.07 km², while the erosion coefficient (Z) showed a gradation in levels from 4.8% for the very severe category with an area of 871.9 km² to 35.8% for the medium category with an area of 6441.8 km². The highest amounts of eroded soil were recorded in the weak erosion category, with a range of 345-573 m³/km²/year and an area of 79,171.6 km². In contrast, the lowest amounts were in the severe erosion category, with a range of (1,210-7,300) m³/km²/year and an area of 3,066.8 km². The study showed that the slope factor, soil quality, and vegetation cover have the greatest impact on water erosion rates.

Through the previous analysis, it was shown that the calcareous loamy soils constitute the largest area with an estimated area of 9.10 km^2 of the basin area, while the second type is the advanced calcareous desert soils, which amounted to an area of 8.15 km^2, and the desert regolith soils constituted the smallest area with an area of 0.68.

The absence of sustainable agricultural practices, coupled with persistent overgrazing pressure, contributes to the undermining of the soil's ability to maintain its surface structure and leads to the destruction of fragile grass and shrub vegetation, making the soil more susceptible to water erosion. Water harvesting or soil conservation techniques exacerbate erosion, particularly in areas with geomorphological features that favor steep surfaces and rapid water runoff.

By establishing reserves for drought-resistant plants such as olives, eucalyptus, cypress, and palm trees, this approach reduces erosion and preserves soil fertility. This is in addition to expanding the cultivation of cereal crops and irrigating them with groundwater, which is available in sufficient quantities and quality for this type of crop. Water harvesting technologies and methods can also be expanded on flat lands, which will increase soil moisture content and promote germination. Contour farming systems can also be adopted in fragile areas. The outputs thus constitute a practical spatial basis that can contribute to formulating sustainable regional strategies for soil and water conservation.

The EPM model is one of the most common models for estimating water erosion due to its simple calculations and flexible application. It can also integrate a range of natural factors, such as rainfall, slope, vegetation cover, and geology, into a comprehensive quantitative equation. This enhances its ability to be employed with remote sensing and GIS techniques to produce accurate spatial maps of erosion and sediment loss. Its importance is particularly evident in arid and semi-arid environments, such as western Iraq, where it compensates for a lack of field data and serves as a scientific tool for planning, land management, and soil protection. However, this model suffers from some limitations that should be taken into account. Some of its parameters rely on

qualitative estimates that may reduce the accuracy of the results. It neglects to distinguish between detailed erosion patterns and is highly sensitive to the accuracy of climate data. It also provides quasi-static estimates that do not reflect temporal changes in erosion unless the application is repeated periodically. Therefore, the model represents a practical and effective tool for estimating erosion and identifying treatment priorities, provided it is supported by local calibration and field data to enhance the reliability of its results. Accordingly, the study recommends the establishment of an integrated spatial database for the basin to support future environmental studies, and the construction of earth and fill dams in the main and secondary channels to retain sediments and invest them in reclaiming new lands, in addition to expanding field studies to characterize soil types and increase the green area.

4. CONCLUSIONS

Morphological and laboratory analyses, based on FAO maps, revealed a clear variation in soil erosion susceptibility as measured by the Y-index. Bulk density ranged from 1.20 to 1.40 mg/cm³, reflecting the different responses of soils to weathering and transport. Consequently, the soils were classified into two groups with varying resistance to erosion.

The soil protection index (Xa) results showed a general decrease in protection levels within areas limited by vegetation cover, particularly in the west. The weak protection category was prevalent, covering a large area of approximately 11,446.9 km², while the very weak protection category was very limited. This highlights the crucial role of vegetation cover in reducing soil erosion susceptibility.

The slope index (Ja) data revealed the dominance of the weak and very weak slope categories across approximately 80% of the region's topography, representing plains and valley bottoms. The steep and very steep slope categories were concentrated in the highlands with active erosion. This pattern is reinforced by the steep slope, sparse vegetation cover, and the nature of the loose material.

The rainfall index (H) shows an average annual rainfall of approximately 125 mm, but its impact is primarily linked to short, high-intensity storms. This pattern contributes to an increased precipitation coefficient within the EPM model and higher soil erosion rates. It also explains the significant spatial variation in erosion intensity within the basin.

Analysis of the temperature index (T) reveals a significant temperature variation from west to east (10.9–37.2°C), influenced by topography and sparse vegetation cover. This temperature increase contributes to higher evaporation and lower soil moisture, promoting soil disintegration and rock weathering. The results demonstrate the role of temperature as a complementary factor that increases soil erosion susceptibility and erosion activity.

REFERENCES

[1] Ramel, K.A., Mehemdi, Y.H.A., Awad, A.Y. (2024). Analysis of the trends of change in temperature and precipitation and their impact on water in Anbar Governorate (1980-2023). Dirasat: Human and Social Sciences, 51(5): 16-32. https://doi.org/10.35516/hum.v51i1.10019

[2] Al-Timimi, Y.K., Al-Lami, A.M., Basheer, F.S., Awad, A.Y. (2024). Impacts of climate change on thermal bioclimatic indices over Iraq. Iraqi Journal of Agricultural Sciences, 55(2): 744-756. https://doi.org/10.36103/j93nst49

[3] Shehab, A.I., Fayyadh, A.F. (2024). The Gavrilovic model to estimate the volume of water erosion in Al-Ratka Valley basin. International Journal of Design & Nature and Ecodynamics, 19(6): 2117-2126. https://doi.org/10.18280/ijdne.190628

[4] Limame, A., Hairchi, K.E., Hanchane, M., Elkhazzan, B., Ouiaboub, L. (2024). Assessment and mapping of water erosion by the integration of Gavrilovic's "EPM" model in the MENA region: Case study of the Admer-Ezem sub-watershed, upper Oum-Rbaa basin, Morocco. Environmental Monitoring and Assessment, 197(1): 40. https://doi.org/10.1007/s10661-024-13470-9

[5] Wu, Q., Jiang, X., Shi, X., Zhang, Y., Liu, Y., Cai, W. (2024). Spatiotemporal evolution characteristics of soil erosion and its driving mechanisms-a case Study: Loess Plateau, China. Catena, 242: 108075. https://doi.org/10.1016/j.catena.2024.108075

[6] Sayel, J.J., Khalaf, A.M., Al-Bayati, A.H.I. (2025). Spatial distribution of some soil characteristics of Ramadi district, western Iraq. International Journal of Environmental Impacts, 8(1): 103-111. https://doi.org/10.18280/ijei.080111

[7] Dragičević, N., Karleuša, B., Ožanić, N. (2018). Modification of Erosion Potential Method using climate and land cover parameters. Geomatics, Natural Hazards and Risk, 9(1): 1085-1105. https://doi.org/10.1080/19475705.2018.1496483

[8] Salma, K., Ahmed, A., Abdellah, A., Salma, E. (2024). Estimation and mapping of water erosion and soil loss: Application of Gavrilovic erosion potential model (EPM) using GIS and remote sensing in the Assif El Mal Watershed, Western high Atlas. China Geology, 7(4): 672-685. https://doi.org/10.31035/cg2023058

[9] Dragičević, N., Karleuša, B., Ožanić, N. (2016). A review of the Gavrilović method (Erosion Potential Method) application. Građevinar, 68(9): 715-725. https://doi.org/10.14256/JCE.1602.2016

[10] Elbadaoui, K., Mansour, S., Ikirri, M., Abdelrahman, K., Abu-Alam, T., Abioui, M. (2023). Integrating erosion potential model (EPM) and PAP/RAC guidelines for water erosion mapping and detection of vulnerable areas in the Toudgha River Watershed of the Central High Atlas, Morocco. Land, 12(4): 837. https://doi.org/10.3390/land12040837

[11] Ali, D.K., Al-Dulaimi, Y.H.O., Jumaa, M.A.R. (2023). The tourism development strategy in the Anbar governorate. Dirasat: Human and Social Sciences, 50(6): 231-245. https://doi.org/10.35516/hum.v50i6.7055

[12] Yassin, A.A., Jubier, A.R., Fazza, A.K. (2025). Spatial modelingg of soill texture classes for Al–Najmi District in Al–Muthanna Governorate using the spatial interpolation method. Anbar Journal of Agricultural Sciences, 23(1): 131-146. https://doi.org/10.32649/ajas.2025.186587

[13] Al-Qayyssi, K.A., Mohammed, K.S., Al-Dulaimi, S.Z., Al-Rawi, M.K., Fayyadh, A.F. (2024). Estimating soil erosion in Al-Aubyth valley using modern techniques and the RUSLE equation. International Journal of Design & Nature and Ecodynamics, 19(5): 1551-1561. https://doi.org/10.18280/ijdne.190509

[14] Marouane, L., Lahcen, B., Valérie, M. (2021). Assessment and mapping of water erosion by the integration of the Gavrilovic "EPM" model in the Inaouene watershed, Morocco. E3S Web of Conference, 314: 03009. https://doi.org/10.1051/e3sconf/202131403009

[15] Haleme, K.G., Al-Dulaimi, S.Z., Razzaq, A.S.A.A., Algayssi, K.A.A.A. (2025). The relationship between large-scale relative vorticity fields and rainfall in Syria during the period, 1980-2020. The Arab World Geographer, 28(1): 62-77. https://doi.org/10.5555/1480-6800-28.1.62

[16] Benaiche, M., Mokhtari, E., Berghout, A. (2024). Assessment of soil erosion in the Boussellam watershed, Algeria: Integrated approach using the Erosion Potential Method (EPM) and GIS. Glasnik Srpskog Geografskog Drustva, 104(1): 113-128. https://doi.org/10.2298/GSGD2401113B

[17] Oroud, I.M., AlTubeiri, Z.S.A. (2023). Estimation of evaporation from the surface water of the Gulf of Aqaba using Band 10 Onboard Landsat 8. Dirasat: Human and Social Sciences, 50(6): 231-243.

[18] Satam, A.T.M., Aldulaimi, A.M.K., Mushref, Z.J. (2022). Assessment of the water environment of the Euphrates River in the district of Fallujah. AIP Conference Proceedings, 2400(1): 040005. https://doi.org/10.1063/5.0112622

[19] Satam, A.T.M., Mukhlef, W.H., Razzaq, A.S.A.A., Mushref, Z.J., Sulaiman, S.O. (2025). Spatial and temporal variations in water quality of the Euphrates River: A sustainable water management approach for Anbar Governorate, Iraq. International Journal of Design & Nature and Ecodynamics, 20(1): 99-106. https://doi.org/10.18280/ijdne.200111

[20] Mohammed, K.S., Al-lahaibi, A.F.F., Abdullah, K.A. (2024). Evaluating temporal variations in soil deterioration in Iraq's Karma district using spectral indicators. Anbar Journal of Agricultural Sciences, 22(2): 1397. https://doi.org/10.32649/ajas.2024.184878